

## Influence of methoxy substitution on flavonoid photophysics: a steady state and laser flash photolysis study

Marcelo Christoff, Vicente G. Toscano, Wilhelm J. Baader \*

*Instituto de Química, Universidade de São Paulo, C.P. 26.077, 05599-970, São Paulo, S.P., Brazil*

Received 27 November 1995; accepted 3 June 1996

### Abstract

A comparative study of the photophysical properties of three flavonoids (flavone (F), 7-methoxyflavone (7MF) and 3-methoxyflavone (3MF)), which may serve as models for naturally occurring flavonoids, shows a distinct behaviour of the 3-methoxy derivative. Steady state and transient spectroscopic investigations reveal an almost quantitative formation of the triplet states of F and 7MF, which can be observed as transient absorptions and show electron donor and acceptor properties. In contrast, 3MF shows reduced triplet formation, and the transient observed is identified as a 1,4-biradical, formed by intramolecular hydrogen abstraction, which behaves as an electron donor.

**Keywords:** Flavonoid photophysics; Laser flash photolysis; Methoxy substitution; Steady state photolysis

### 1. Introduction

Flavonoids are a large class of natural pigments which contain the flavone unit (2-phenyl-4-benzopyrone) in their structure. These compounds are usually found in the tissues of higher plants, mainly in the tropical regions [1]. Flavonoid biosynthesis is photomodulated by UV and blue radiation at different points [2]. The efficient absorbance of the flavonoids (coefficient of molar absorptivity,  $\epsilon \sim 10^4 \text{ M}^{-1} \text{ cm}^{-1}$  [3]) in the range 290–400 nm (cinnamoyl part) and 240–285 nm (benzoyl part) has implied their possible involvement in the protection against UV-induced damage in plants [4–7].

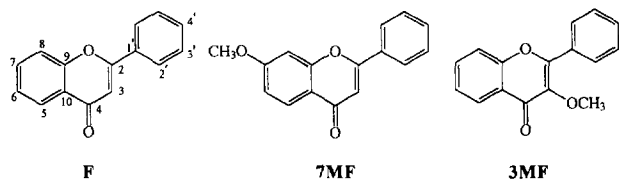
Photophysical and photochemical studies on flavonoids have revealed important characteristics which may be related to their photobiological behaviour. Studies of the photochemical behaviour of flavone have shown that dimerization is the main photoreaction of the parent derivative [8]. In micellar medium, the photochemistry of flavone is influenced by the polarity and charge of the micellar surface [9]. Employing time-resolved spectroscopic techniques, Hamanoue et al. [10] observed ultrafast intersystem crossing (ISC) ( $k_{\text{ISC}} = 10^{12} \text{ s}^{-1}$ ) in flavone, in agreement with its lack of fluorescence in aprotic media. These findings suggest that the photochemistry of flavone is mainly mediated by its triplet excited state, as confirmed by the high ISC yield ( $\Phi_{\text{ISC}} \sim 0.9$ )

[11]. The transient absorption spectrum of triplet flavone has been recorded with bands at 365–370 nm (maximum) and 640–650 nm [10–12]. The effect of the solvent polarity on the lifetime of this transient indicates a  $\pi, \pi^*$  character for the lowest triplet excited state of flavone [10]. The flavone triplet is quenched by several typical triplet quenchers and is reactive towards hydrogen donors [11]. Similar results were obtained in a study on the photoreduction of flavone by several amines in homogeneous solution and micellar systems [12].

The photochemistry of 3-hydroxyflavone in solution results in photorearrangement products [13]. Using time-resolved fluorescence and flash photolysis, a tautomeric transient generated by intramolecular proton transfer and involving the singlet excited state was identified [14–17]. Under similar conditions, analogous transients were observed from polysubstituted 3-hydroxyflavone derivatives [18] and other monohydroxyflavones [19,20]. These examples demonstrate the strong changes in the photophysical and photochemical behaviour of flavone in the presence of hydroxy substituents. Recent studies on chalcone derivatives of natural occurrence have also shown the modulation of the excited state behaviour by the substitution pattern [21].

In order to identify the influence of methoxy substituents on flavone excited state behaviour, a family of these molecules, including natural derivatives, has been investigated in our laboratory. In this paper, we report a comparative study, involving steady state and transient absorption spectroscopy,

\* Corresponding author. Tel.: +55 11 8183877; fax: +55 11 8155579.



Scheme 1. Structures of flavone (F), 7-methoxyflavone (7MF) and 3-methoxyflavone (3MF).

of simple methoxy-substituted flavones and parent flavone (flavone (F), 7-methoxyflavone (7MF) and 3-methoxyflavone (3MF), see Scheme 1). The nature of the lowest excited singlet and triplet states was identified, and the reactivity of transients, generated by flash photolysis, towards energy and electron acceptors and donors was determined. The results show significant changes in the photophysical and photochemical behaviour of the flavones on introduction of a methoxy group in the 3-position.

## 2. Experimental details

### 2.1. Materials

Acetonitrile (ACN) was purified following the literature procedure [22], and cyclohexane (CH) and methylcyclohexane (MCH) spectral grade (Aldrich Gold Label) were used as received. Tetracyanoethylene (TCNE) (Aldrich), 9,10-diphenylanthracene (DPA) (Aldrich) and 1,4-diazabicyclo[2.2.2]octane (DABCO) (Aldrich) were purified by sublimation (1 mmHg). Benzophenone (BZP) (Aldrich) and 1,1'-dimethyl-4,4'-bipyridinium chloride ( $MV^{2+}$ ) (Aldrich) were recrystallized from ethanol and methanol respectively. 2,5-Dimethyl-2,4-hexadiene (DMH) (Chemical Samples Co.), 1,3-cyclohexadiene (CHD) (Chemical Samples Co.) and F (Aldrich) were used as received. The methoxyflavones were obtained by methylation of the corresponding hydroxyflavones (Aldrich) in the presence of an excess of diazomethane (7MF) or dimethylsulphate (3MF). The methoxyflavones were recrystallized at least three times from CH. The  $^1H$  (Bruker AC-200-F, 200.1 MHz) and  $^{13}C$  (50 MHz) nuclear magnetic resonance (NMR) spectra of these methoxyflavones in dimethylsulphoxide- $d_6$  (DMSO- $d_6$ ) are in agreement with the literature [23], and clearly indicate the introduction of a methoxy carbon (3MF:  $^1H$ , 3.81 ppm;  $^{13}C$ , 59.9 ppm; 7MF:  $^1H$ , 3.92 ppm;  $^{13}C$ , 56.2 ppm), as well as the disappearance of the hydroxy hydrogen (3MF:  $^1H$ , 9.62 ppm; 7MF:  $^1H$ , 8.73 ppm).

3MF:  $^{13}C$  NMR (DMSO- $d_6$ , 50 MHz, ppm): O-CH<sub>3</sub>, 59.9; C-2, 154.9; C-3, 140.9; C-4, 171.1; C-5, 125.1; C-6, 125.3; C-7, 134.3; C-8, 118.6; C-9, 155.2; C-10, 123.7; C-1', 130.6; C-2', 128.5; C-3', 128.9; C-4', 131.1.

7MF: C-2, 162.6 ppm; F: C-2, 163.2 ppm [23].

### 2.2. Methods

Unless otherwise stated, all experiments were performed at 298 K.

#### 2.2.1. Oxidation potentials

The half-wave oxidation potentials ( $E_{1/2ox}$ ) were measured by cyclic voltammetry in ACN (vs. Ag/AgI; with supporting electrolyte NaClO<sub>4</sub> (0.1 M) and working electrode Pt/Pt) to be 2.19 eV and 2.50 eV for 3MF and 7MF respectively. F does not show oxidation up to 2.80 eV ( $E_{1/2ox}$  of ACN).

#### 2.2.2. Steady state spectroscopic measurements

Absorption spectra were recorded in rectangular quartz cells (10 mm × 10 mm, 3 ml) on a Hitachi 2000 spectrophotometer and emission spectra on a SPEX Fluorolog 1681 fluorometer. Emission spectra were corrected for monochromator and photomultiplier response. The fluorescence quantum yields were determined in ACN and CH using DPA as standard and utilizing solutions with absorptions between 0.02 and 0.05 at  $\lambda_{exc}$ . The phosphorescence quantum yields were determined in MCH and ethanol–isopentane–ether (2 : 5 : 5) (EPA) glasses, using naphthalene and BZP as standards respectively (absorptions between 0.02 and 0.05 at  $\lambda_{exc}$ ), and employing quartz tubes with a diameter of 0.5 mm. All phosphorescence measurements were performed at 77 K.

#### 2.2.3. Laser photolysis measurements [24]

Laser measurements were obtained using an Applied Photo-physics fast kinetics transient photometer operating with 15 ns full width at half-maximum (FWHM) of Nd-YAG harmonics at 355 nm (third; around 20 mJ per pulse) or 266 nm (fourth; around 6 mJ per pulse). A pulsed xenon lamp was used as the monitoring beam at an observation angle of 90°. The decay kinetics were monitored following the disappearance of the transient absorption at suitable wavelengths with a Tektronix 2230 100 MHz digitizer. The digitizer signals were transferred to an IBM microcomputer and analysed by first-order decay kinetics. The transient absorption spectra were obtained point by point at the time window indicated. Solutions in rectangular quartz cells were deaerated by argon bubbling for 20 min and their concentration was checked prior to photolysis. All rate constants determined by time-resolved techniques are accurate to  $\pm 15\%$ .

#### 2.2.4. Conventional photolysis measurements

3MF (21 mM) was irradiated in ACN with a 450 W medium pressure Hg lamp (313 nm) for 24 h in a quartz tube with argon bubbling. Fractions of 1 ml were collected at the times indicated and analysed by spectrophotometry at suitable dilutions. The solvent was evaporated from the final reaction mixture and the product mixture was analysed by  $^1H$  and  $^{13}C$  NMR in DMSO- $d_6$ . Distortionless enhancement by polarization transfer (DEPT) experiments were performed using standard Bruker software.

The main photoproduct was isolated from the final photolysis product mixture by preparative thin layer chromatography (TLC) on silica gel (TLC standard grade) using CHCl<sub>3</sub>–methanol (98 : 2) as mobile phase. The product at

$R_F = 0.47$  was extracted from the silica gel with  $\text{CH}_2\text{Cl}_2$  and, after solvent evaporation, a slightly yellow oil was obtained.

$^{13}\text{C}$  NMR (DMSO- $d_6$ , 50 MHz, ppm):  $^1$ : O- $\text{CH}_2$ , 67.0; C-2, 148.6<sup>2</sup>; C-3, 147.5<sup>2</sup>; C-4, 170.3<sup>2</sup>; C-5, 124.4; C-6, 124.5; C-7, 133.3; C-8, 117.9; C-9, 153.9<sup>2</sup>; C-10, 121.4<sup>2</sup>; C-1', 137.6<sup>2</sup>; C-2', 131.2; C-3', 127.3; C-4', 128.2; C-5', 131.2; C-6', 124.7<sup>3</sup>.

### 3. Results

#### 3.1. Steady state spectroscopy

The long-wavelength maxima ( $\lambda_{\text{max}}^{\text{A}}$ ) in the absorption spectra of 3MF and 7MF show a red shift relative to that of F in ACN and CH (Fig. 1, Table 1). This effect, expected due to the electron-donating effect of the methoxy group, is more pronounced for 7MF than for 3MF, i.e. 11 nm vs. 5 nm respectively in ACN. The position of the low energy shoulder ( $\lambda_{\text{sh}}^{\text{A}}$ ) of the long-wavelength band shows distinct shifts for the methoxyflavones in relation to F; in CH, a 4 nm hypsochromic shift is observed for 3MF, whereas 7MF shows a 12 nm bathochromic shift (Fig. 1, Table 1). An increase in the solvent polarity promotes a red shift of all  $\lambda_{\text{max}}^{\text{A}}$  values, which is larger for 7MF than for F and 3MF, so that the shoulder disappears in the case of 7MF (Fig. 1(B), Table 1). The maximum molar absorptivity coefficients ( $\epsilon_{\text{max}}^{\text{A}}$ ) increase with increasing solvent polarity; 7MF shows the smallest change (Table 1).

F and 7MF do not show measurable fluorescence emission in polar aprotic and apolar solvents. In contrast, 3MF shows fluorescence emission even in MCH ( $\Phi_f < 0.01$ ), which is significantly enhanced in ACN ( $\Phi_f = 0.03$ ) (Table 1). Ormson et al. [25] have reported similar values for  $\Phi_f$  of 3MF in MCH and ACN (0.01 and 0.02 respectively), as well as the energy of the lowest singlet excited state ( $E_{\text{S}_1}$ ).

<sup>1</sup> The assignments of the signals should be considered preliminary.

<sup>2</sup> The signals of these quaternary carbons could only be observed in  $\text{C}_6\text{D}_6$  due to the higher solubility of the photoproduct in this solvent.

<sup>3</sup> Signals due to unidentified impurities were observed at 120.1, 121.1 and 127.9 ppm.

Table 1  
Steady state spectroscopic data<sup>a</sup>

| Parameter  | F              | 7MF            | 3MF             |
|--|----------------|----------------|-----------------|
| Absorption   |                |                |                 |
| $\lambda_{\text{max}}^{\text{A}}, \lambda_{\text{sh}}^{\text{A}}, \log \epsilon_{\text{max}}^{\text{A}}$ (ACN) | 289, 302, 4.28 | 300, 4.36      | 294, 315, 4.24  |
| $\lambda_{\text{max}}^{\text{A}}, \lambda_{\text{sh}}^{\text{A}}, \log \epsilon_{\text{max}}^{\text{A}}$ (CH)  | 286, 302, 4.12 | 293, 298, 4.33 | 291, 315, 4.14  |
| Fluorescence   |                |                |                 |
| $\lambda_{\text{max}}^{\text{f}}, E_{\text{S}_1}^{\text{f}}, \Phi_{\text{f}}$ (ACN)                            | c              | c              | 410, 73, 0.03   |
| $\lambda_{\text{max}}^{\text{f}}, E_{\text{S}_1}^{\text{f}}, \Phi_{\text{f}}$ (CH)                             | c              | c              | 419, 74, <0.01  |
| Phosphorescence <sup>d</sup>   |                |                |                 |
| $\lambda_{\text{max}}^{\text{ph}}, E_{\text{T}_1}^{\text{ph}}, \Phi_{\text{ph}}$ (EPA)                         | 469, 63, 1.00  | 469, 63, 0.89  | c               |
| $\lambda_{\text{max}}^{\text{ph}}, E_{\text{T}_1}^{\text{ph}}, \Phi_{\text{ph}}$ (MCH)                         | 465, 64, 0.76  | 465, 64, 0.75  | 465, 69, <<0.01 |

<sup>a</sup>Wavelengths (nm);  $\epsilon$  ( $\text{M}^{-1} \text{cm}^{-1}$ ). <sup>b</sup>Units:  $\text{kcal mol}^{-1}$ . <sup>c</sup>Not detected. <sup>d</sup>At 77 K.

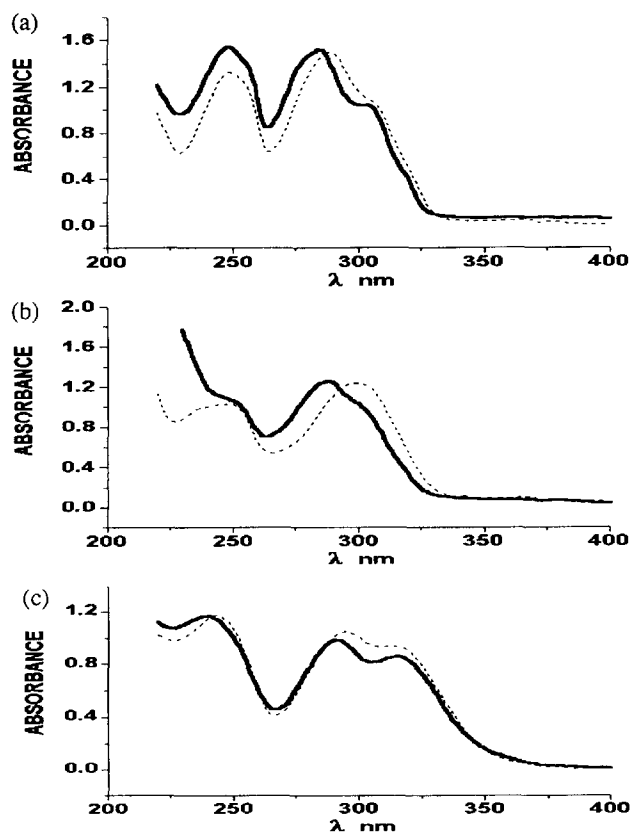


Fig. 1. Absorption spectra of F, 7MF and 3MF in polar and apolar solvents: (A) F, 80  $\mu\text{M}$  in ACN (---), 115  $\mu\text{M}$  in CH (—); (B) 7MF, 55  $\mu\text{M}$  in ACN (---), 50  $\mu\text{M}$  in CH (—); (C) 3MF, 60  $\mu\text{M}$  in ACN (---), 70  $\mu\text{M}$  in CH (—).

However, F and 7MF show phosphorescence quantum yields ( $\Phi_{\text{ph}}$ ) of almost unity in EPA glass and only slightly reduced yields in MCH glass (Table 1). In contrast, 3MF phosphorescence is not detectable in EPA glass and only very weak in MCH glass (Fig. 2). The triplet energies ( $E_{\text{T}_1}$ ), estimated from the onset of the phosphorescence spectra in MCH, show similar values for 7MF and F ( $64 \text{ kcal mol}^{-1}$ ) and a slightly higher value for 3MF ( $69 \text{ kcal mol}^{-1}$ ) (Table 1). In reasonable agreement, Bhattacharyya et al. [11] have reported a value of  $62 \text{ kcal mol}^{-1}$  for  $E_{\text{T}_1}$  of F in benzene.

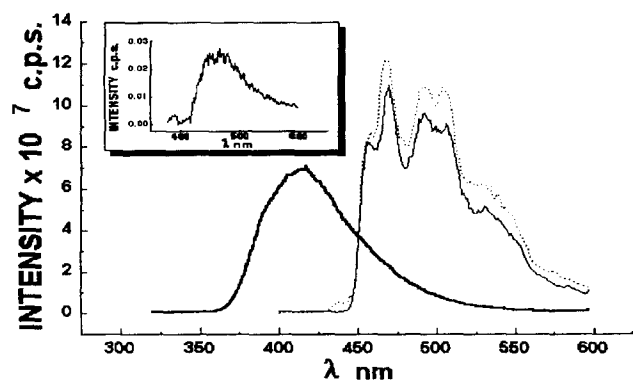


Fig. 2. Emission spectra of F, 7MF and 3MF. Phosphorescence spectra of F (91  $\mu\text{M}$  in EPA glass, excitation at 303 nm) (---) and 7MF (73  $\mu\text{M}$  in EPA glass, excitation at 326 nm) (—). Fluorescence spectrum of 3MF (120  $\mu\text{M}$  in EPA glass, excitation at 301 nm) (—). Inset: phosphorescence spectrum of 3MF (25  $\mu\text{M}$  in MCH glass, excitation at 343 nm). All spectra were obtained at 77 K.

The results given above indicate an almost complete conversion of the lowest singlet states of F and 7MF to the triplet states in both polar and apolar solvents. At 77 K, these triplets are preferentially deactivated by phosphorescence emission and the total radiative quantum yield ( $\Phi_{\text{rd}} = \Phi_{\text{f}} + \Phi_{\text{ph}}$ ) is almost unity. In contrast, the total radiative quantum yield of 3MF is less than 0.05, which indicates efficient non-radiative deactivation of the excited singlet or triplet states of 3MF.

### 3.2. Transient absorption spectroscopy

#### 3.2.1. F and 7MF

Deaerated F and 7MF solutions (approximately  $10^{-4}$  M) in ACN produce very similar transient absorption spectra on laser flash photolysis (Nd:YAG; 266 nm), with a single band and maximal absorption at  $\lambda_{\text{max}}^{\text{T}}$  of about 370–375 nm (Fig. 3(A) and Fig. 3(B)). The insets in Fig. 3(A) and Fig. 3(B) show first-order decay kinetics of these transients, with lifetimes ( $\tau_{\text{d}}$ ) of around 5  $\mu\text{s}$  (Table 2). The apparent first-order rate constants ( $k$ ) increase with increasing flavonoid concentration, giving self-quenching rate constants ( $k_{\text{sq}}$ ) of approximately  $10^8 \text{ M}^{-1} \text{ s}^{-1}$  (Table 2), relatively close to the reported value of  $8 \times 10^7 \text{ M}^{-1} \text{ s}^{-1}$  [11]. The molar absorptivity coefficients ( $\epsilon_{\text{max}}^{\text{T}}$ ) of the F and 7MF transients at 370 nm were determined to be 10 000 and 8000  $\text{M}^{-1} \text{ cm}^{-1}$  respectively using BZP as standard ( $\epsilon_{\text{max}}^{\text{T}} = 7870 \text{ M}^{-1} \text{ cm}^{-1}$  at 530 nm) [26]. Similar values were reported for the triplet transient of F in benzene [11] and ACN [12].

#### 3.2.2. 3MF

The transient generated by excitation of 3MF (266 or 355 nm) shows  $\lambda_{\text{max}}^{\text{T}} = 440 \text{ nm}$  (Fig. 3) and complex kinetic behaviour. In the region of maximal absorption (420–460 nm), the transient shows a biexponential decay (curve 1, inset of Fig. 3(C)) with lifetimes of about 4  $\mu\text{s}$  and greater than 20  $\mu\text{s}$  (Table 2). Only the fast decay component is observed at the borders of the absorption spectrum (360 or 520 nm, curve 2, inset of Fig. 3(C)). No self-quenching is

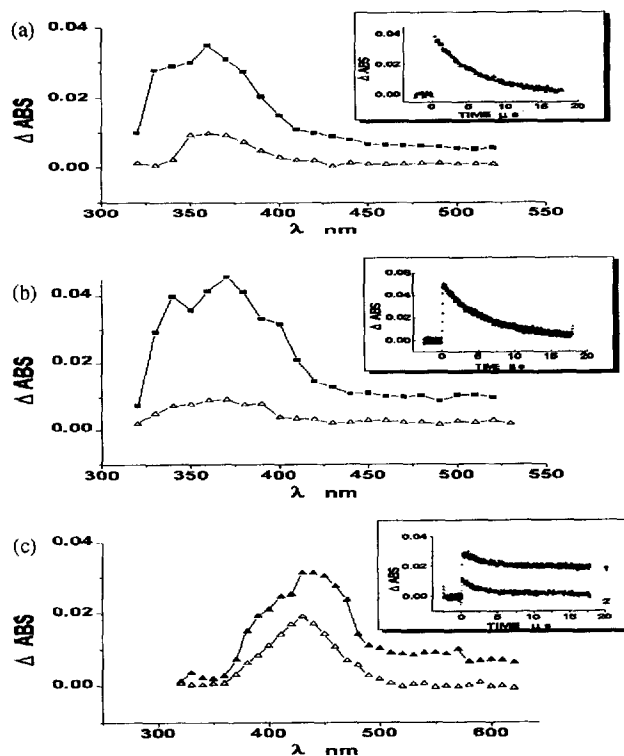


Fig. 3. Transient absorption spectra and decay kinetics (inset) of F, 7MF and 3MF in ACN: (A) F, 110  $\mu\text{M}$ ; inset, 370 nm; (B) 7MF, 80  $\mu\text{M}$ ; inset, 370 nm; (C) 3MF, 112  $\mu\text{M}$ ; inset: (1) 430 nm; (2) 500 nm. These spectra were obtained 0.5  $\mu\text{s}$  (upper) and 8  $\mu\text{s}$  (lower) after the laser pulse (266 nm, 6 mJ).

observed for the 3MF transient and  $\epsilon_{\text{max}}^{\text{T}}$  at 440 nm was determined to be  $6000 \text{ M}^{-1} \text{ cm}^{-1}$ .

### 3.3. Physical quenching and triplet sensitization

#### 3.3.1. F and 7MF

The transients from F and 7MF were completely quenched by oxygen ( $1.9 \times 10^{-3} \text{ M}$ ) [27] in ACN. The physical quenching of the F and 7MF transients by CHD ( $E_{\text{T1}} = 52 \text{ kcal mol}^{-1}$ ) [27] and DMH ( $E_{\text{T1}} = 55 \pm 2 \text{ kcal mol}^{-1}$ )<sup>4</sup> was measured at the respective maximum absorptions; from the linear plots of the inverse of the transient lifetime vs. the quencher concentration (Fig. 4), quenching rate constants ( $k_{\text{p}}$ ) of around  $4 \times 10^9 \text{ M}^{-1} \text{ s}^{-1}$  were obtained (Table 2), close to the diffusion-controlled limit in ACN ( $1.9 \times 10^{10} \text{ M}^{-1} \text{ s}^{-1}$ ) [27]. Bhattacharyya et al. [11] reported a rate constant of  $4.9 \times 10^9 \text{ M}^{-1} \text{ s}^{-1}$  for the quenching of the F triplet by DMH, in good agreement with our values.

Triplet sensitization by BZP ( $E_{\text{T1}} = 69 \text{ kcal mol}^{-1}$ ) for F and 7MF ( $\lambda_{\text{ex}} = 355 \text{ nm}$ ) in ACN generates transients with

<sup>4</sup> A value of 42  $\text{kcal mol}^{-1}$  is reported in the literature [27]; however, this energy corresponds to the equilibrium triplet state after relaxation [28]. As DMH is used as quencher in our work, the energy of the Franck–Condon triplet should be used. A value of  $E_{\text{T}} = 58.7 \text{ kcal mol}^{-1}$  in a non-polar solvent has been reported [29], but this value appears to be too high. From a more recent careful quenching study in benzene [28], a value of  $E_{\text{T}} = 55 \pm 2 \text{ kcal mol}^{-1}$  can be extracted as the most reasonable triplet energy for DMH.

Table 2  
Flash photolysis data<sup>a</sup>

| Parameter  | F            | 7MF          | 3MF                           |
|--|--------------|--------------|-------------------------------|
| <b>Transient absorption</b>                                  |              |              |                               |
| $\lambda_{\max}^T$ (nm), $\log \epsilon_{\max}^T$            | 370, 4.0     | 375, 3.8     | 440, 3.2                      |
| $k_{AS}^D$ , $\tau_d$ ( $\mu$ s)                             | 0.2, 5.1     | 0.8, 5.6     | <sup>c</sup> , 4 <sup>d</sup> |
| <b>Physical quencher</b>                                     |              |              |                               |
| 1,3-Cyclohexadiene, $k_{PC}^b$ , $\tau_{PC}^e$ ( $\mu$ s)    | 3.6, 4.2     | 4.2, 3.6     | <sup>c</sup>                  |
| 2,5-Dimethylhexadiene, $k_{PD}^b$ , $\tau_{PD}^e$ ( $\mu$ s) | 4.3, 3.8     | 4.7, 3.4     | <sup>c</sup>                  |
| <b>Energy donor</b>  |              |              |                               |
| Benzophenone, $k_{PB}^b$                                     | 9.2          | 4.8          | <sup>c</sup>                  |
| <b>Electron acceptor</b>                                     |              |              |                               |
| TCNE, $k_{EA}^f$ , $\tau_e^g$ ( $\mu$ s)                     | 6.1, 5.6     | 11.1, 3.5    | 9.4, 4.5                      |
| MV <sup>2+</sup> , $k_{EA}^f$ , $\tau_e^g$ ( $\mu$ s)        | <sup>g</sup> | <sup>g</sup> | 0.5, 4.8                      |
| <b>Electron donor</b>  |              |              |                               |
| DABCO, $k_{ED}^h$ , $\tau_e^g$ ( $\mu$ s)                    | 1.2, 5.8     | 2.0, 3.7     | <sup>c</sup>                  |

<sup>a</sup>Solutions in deaerated acetonitrile, excited by 266 nm (Nd/YAG) (6 mJ per pulse). <sup>b</sup>All constants expressed in  $\times 10^{-9}$  ( $M^{-1} s^{-1}$ ). <sup>c</sup>Not observed. <sup>d</sup>Monoexponential decay at the spectrum border and fast component of the biexponential decay at the spectral maximum. <sup>e</sup>Lifetime estimated from the ordinate intercept of the Stern–Volmer plot. <sup>f</sup>Excited at 355 nm (Nd/YAG) (20 mJ per pulse). <sup>g</sup>Not measured (see text).

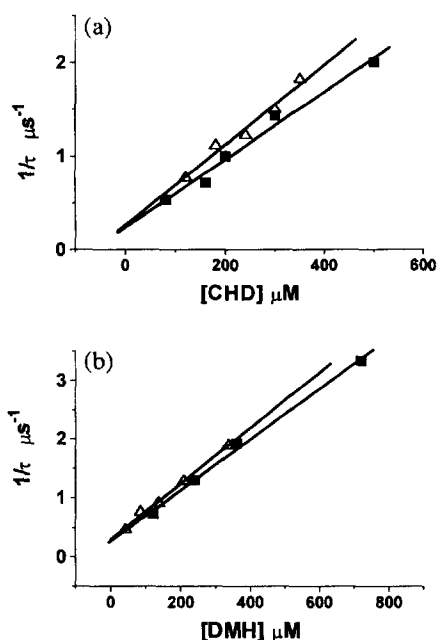


Fig. 4. Stern–Volmer plots for the quenching of the F and 7MF transients by CHD and DMH in ACN: (A) CHD: F, 110  $\mu$ M (■); 7MF, 80  $\mu$ M ( $\Delta$ ); (B) DMH: F, 67  $\mu$ M (■); 7MF, 61  $\mu$ M ( $\Delta$ ). Excitation, 266 nm; observation, 370 nm.

the same characteristics as those generated by direct irradiation. The rate constants for quenching of the BZP triplet ( $k_{PB}$ ) by F and 7MF, determined by monitoring the decay kinetics at 530 nm (absorption maximum of triplet BZP), are  $9.2 \times 10^9 M^{-1} s^{-1}$  and  $4.8 \times 10^9 M^{-1} s^{-1}$  respectively. Bhattacharyya et al. [11] reported a somewhat lower value of  $4.0 \times 10^9 M^{-1} s^{-1}$  for the rate constant of BZP triplet quenching by F in benzene.

### 3.3.2. 3MF

The oxygen quenching of 3MF transients is only partial, eliminating the fast decay component, but causing only a small reduction in the signal intensity of the slow component,

without alteration of its decay constant. No quenching is observed with CHD and DMH.

Due to competitive absorption of BZP and 3MF, it was not possible to verify energy transfer from the BZP triplet to 3MF. The transients generated in various mixtures of BZP and 3MF (BZP,  $10^{-3}$ – $10^{-2}$  M; 3MF,  $10^{-5}$ – $10^{-4}$  M) were the sum of the transients observed on irradiation of each single component under identical conditions (not shown). Moreover, in the 3MF concentration range used ( $10^{-5}$ – $3 \times 10^{-4}$  M), no quenching was observed on monitoring the triplet BZP absorption at 530 nm.

## 3.4. Electron transfer

### 3.4.1. F and 7MF

The transients of F and 7MF were efficiently quenched by the electron donor DABCO ( $E_{1/2ox} = -0.68$  eV vs. saturated calomel electrode (SCE)) [30] concomitantly with the formation of a long-lived transient (Fig. 5 ~ (A)). The transient spectrum appears to be a combination of the DABCO cation radical ( $\lambda_{\max} = 500$  nm) [31] and the 7MF ketyl radical ( $\lambda_{\max} = 370$  nm) absorptions. The latter could be formed by fast protonation of the respective anion radical. Similar spectra were registered in the reductive quenching of triplet F by amines in benzene [11] or ACN [12]. The bimolecular rate constants for quenching of the F and 7MF transients by the electron donor DABCO ( $k_{ED}$ ) are  $1.3 \times 10^9$  and  $2.0 \times 10^9 M^{-1} s^{-1}$  respectively (Table 2), and were obtained from the slopes of the plots of the apparent first-order rate constants vs. the DABCO concentration (Fig. 5(A), inset). In good agreement, the rate constants for reductive quenching of triplet F by triethylamine in benzene and by dimethylamine in ACN were reported to be  $k_{ED} = 3.6 \times 10^8 M^{-1} s^{-1}$  [11] and  $k_{ED} = 2.6 \times 10^9 M^{-1} s^{-1}$  [12] respectively.

In the presence of the electron acceptor TCNE ( $E_{1/2red} = 0.24$  eV vs. SCE) [32], the transients of F and 7MF were quenched, generating long-lived transients with a broad

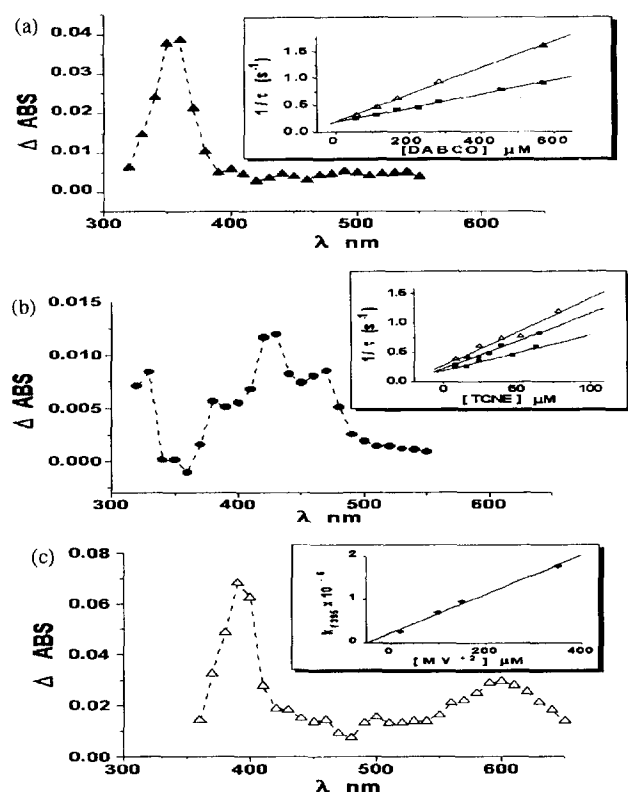


Fig. 5. Transient spectra and Stern–Volmer plots for the electron transfer quenching of the F, 7MF and 3MF transients in ACN: (A) spectrum of 7MF–DABCO 8  $\mu$ s after the pulse; inset, Stern–Volmer plots observed at 330 nm for F (73  $\mu$ M) (bottom) and 7MF (61  $\mu$ M) (top); [DABCO] = 57–570  $\mu$ M; (B) spectrum of F–TCNE 8  $\mu$ s after the pulse; inset, Stern–Volmer plots observed at 370 nm for F (73  $\mu$ M) (bottom) and 7MF (61  $\mu$ M) (top) or at 360 nm for 3MF (56  $\mu$ M) (middle); [TCNE] = 10–70  $\mu$ M; (C) spectrum of 3MF–MV<sup>2+</sup> 3  $\mu$ s after the pulse; inset, plots of  $k_r$  at 395 nm (MV<sup>2+</sup>) vs. [MV<sup>2+</sup>] (20–350  $\mu$ M) for 3MF (142  $\mu$ M). Laser excitation pulse at 266 nm (6 mJ) in (A) and (B) and at 355 nm (20 mJ) in (C).

maximum at 420–430 nm and a shoulder at 450 nm (Fig. 5(B)). Mataga et al. [33] assigned the 420 nm absorption to the radical anion of TCNE; therefore the absorption at 450 nm may be related to the flavone cation radical. The bimolecular rate constants for quenching of the F and 7MF transients by the electron acceptor TCNE ( $k_{EA}$ ) were determined by monitoring the transient decays at 360 nm (Fig. 5(B), inset). This observation wavelength was chosen to avoid interference from the absorption of quenching products. The values of  $k_{EA}$  obtained for F and 7MF ( $6.1 \times 10^9$  and  $11.0 \times 10^9$   $M^{-1} s^{-1}$  respectively, Table 2) are close to the diffusion-controlled limit in ACN ( $1.9 \times 10^{10}$   $M^{-1} s^{-1}$ ) [27]. The electron acceptor MV<sup>2+</sup> ( $E_{Pred} = 0.45$  eV vs. SCE) [34] could not be used with F and 7MF because it shows strong absorption at 266 nm (fourth harmonic of the Nd-YAG laser) and these flavonoids do not absorb at 355 nm (third harmonic of the Nd-YAG laser).

#### 3.4.2. 3MF

Under the same conditions as employed for F and 7MF, no effect was observed on the 3MF transient in the presence of the electron donor DABCO. On the other hand, the fast

component of the 3MF transient was quenched by both electron acceptors employed. From the slope of the plot of the apparent first-order decay constant (at 360 nm) vs. the TCNE concentration (Fig. 5(B), inset), a value of  $k_{EA} = 8.5 \times 10^9$   $M^{-1} s^{-1}$  was obtained (Table 2).

The second electron acceptor MV<sup>2+</sup> was studied using 355 nm excitation (20 mJ) for which direct excitation of MV<sup>2+</sup> is minimal. Quenching of the 3MF transient by MV<sup>2+</sup> results in a transient absorption spectrum containing bands at 395 and 600 nm, with shoulders at 420–470 and 500–550 nm (Fig. 5(C)). The short- and long-wavelength bands can be attributed to the methylviologen monocation radical (MV<sup>•+</sup>), reported in the literature to show absorption at 395 and 603 nm [35]. By analogy with the assignment in the F–TCNE spectrum (Fig. 5(B)), the shoulder at 420–470 nm can be associated with the absorption of the 3MF radical cation and the shoulder at 500–550 nm is probably a residual absorption of MV<sup>•+</sup>. The bimolecular rate constant for quenching of 3MF by MV<sup>2+</sup> was obtained from a plot of the formation rate constant ( $k_r$ ) at 395 nm vs. the MV<sup>2+</sup> concentration (inset, Fig. 5(C)), yielding a value of  $5 \times 10^8$   $M^{-1} s^{-1}$  (Table 2).

#### 3.5. Conventional photolysis of 3MF

Since the transient absorption spectrum of 3MF indicates the formation of a long-lived species, i.e. photochemical transformation of this flavone, some preliminary conventional photolysis studies were undertaken. A solution of 3MF ( $2.1 \times 10^{-2}$  M) in ACN was irradiated at 313 nm (medium pressure Hg lamp, 450 W) under argon at 298 K for 24 h. The UV spectrum obtained during irradiation shows a significant red shift of the low energy band from 291 to 3087 nm, a broadening of this band and a decrease in  $\epsilon_{max}$  (Fig. 6).

Analytical TLC (SiO<sub>2</sub>, CHCl<sub>3</sub>–methanol (98 : 2)) reveals the gradual disappearance of 3MF ( $R_F = 0.56$ ), and the appearance of a prominent photoproduct ( $R_F = 0.47$ ), as well as several other minor products ( $R_F = 0.10$ –0.25). Preliminary analysis of the final product mixture by <sup>1</sup>H and <sup>13</sup>C NMR spectroscopy clearly shows the disappearance of the signals corresponding to the 3-methoxy group (<sup>1</sup>H, 3.82 ppm; <sup>13</sup>C,

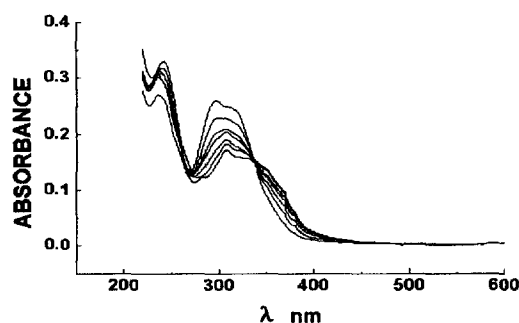


Fig. 6. Absorption spectra of 3MF solutions in ACN, irradiated at 313 nm (medium pressure Hg lamp, 450 W). Samples collected during photolysis at 1, 2, 3, 4, 5, 6 and 24 h (from top to bottom). 3MF (21 mM) solution diluted 140 times to obtain the spectra.

59.9 ppm) and the appearance of signals compatible with an ethereal methylene group ( $^1\text{H}$ , 5.29 ppm;  $^{13}\text{C}$ , 67.0 ppm). The DEPT spectrum confirms the assignment of the 67.0 ppm signal to a  $\text{CH}_2$  group (inversion of peak polarization relative to the CH groups).

NMR spectroscopy of the main photoproduct ( $R_F=0.47$ ), partially purified by preparative TLC, confirms the complete transformation of the methoxy to an ethereal methylene group. The assignment of the  $^{13}\text{C}$  NMR spectrum of this photoproduct is given in Section 2. A preliminary analysis of the rather complex  $^1\text{H}$  NMR spectrum of the photoproduct, in comparison with that of 3MF, shows that the signals of the pyranone ring protons are largely maintained in the product spectrum. However, the signals corresponding to the 2-phenyl protons (2', 6' and 3', 5' appear as a superimposed multiplet for 3MF) show a considerable change and appear at distinct chemical shift values (data not shown), indicating a substitution at the phenyl group.

## 4. Discussion

### 4.1. Steady state spectroscopic studies

Steady state spectroscopic studies of the flavones suggest a distinct behaviour of 3MF relative to F and 7MF with respect to the excited state deactivation channels. Optical and magnetic resonance studies [36] have established that the low-lying  $\pi, \pi^*$  and  $n, \pi^*$  configurations of chromone (4-benzopyrone) are nearly isoenergetic and very strongly mixed. Considering only the electron donor effect of the methoxy group, an increase in the  $\pi, \pi^*$  character of the lowest singlet excited state ( $S_1$ ) of the methoxyflavones relative to the dominant  $n, \pi^*$  character in F [10] is expected. Accordingly, the absorption spectrum of 7MF clearly shows a red shift in  $\lambda_{\text{max}}^A$  and an increase in  $\epsilon_{\text{max}}^A$  in comparison with F, which is characteristic of an increase in the  $\pi, \pi^*$  nature of  $S_1$ . The analogous parameters in the absorption spectrum of 3MF show only small changes (Table 1). A possible explanation for the more pronounced electron donor effect in 7MF relative to 3MF may be the lower electron density in ring A compared with the pyrone ring, which is expected to be electron rich due to the presence of the heterocyclic and carbonyl oxygen. Preliminary results of semi-empirical calculations support this assumption [37].

In addition, the long-wavelength shoulder ( $\lambda_{\text{sh}}^A$ ) in the spectrum of F, due to the  $n \rightarrow \pi^*$  transition, is blue shifted and considerably reduced in intensity (in CH) or not observed (in ACN) for 7MF, facts which indicate a minor contribution of the  $n \rightarrow \pi^*$  transition in 7MF. Consequently, the red shift observed for  $\lambda_{\text{sh}}^A$  of 3MF can be interpreted as an increase in the  $n \rightarrow \pi^*$  nature of the 3MF transition. The solvent effect also corroborates these assignments; a decrease in polarity leads to a blue shift of  $\lambda_{\text{max}}^A$ , dominated by the  $\pi \rightarrow \pi^*$  transition, as well as an increase in  $\lambda_{\text{sh}}^A$ , indicating increasing  $n, \pi^*$  character (Table 1). The unusual effect of

the methoxy group on the photophysical properties of 3MF can be understood by considering a loss of resonance between the 2-phenyl group and the benzopyrone moiety, resulting from the steric repulsion between the 3-methoxy and the 2-phenyl groups. Additionally, the interaction of the 3-methoxy oxygen lone pair with the carbonyl group may contribute to the decrease in the energy of the  $n, \pi^*$  singlet state.

The emission characteristics of the flavones are also influenced by 7- and 3-methoxy substitution. Similar to F, 7MF shows  $\Phi_{\text{ph}}$  of almost unity and no fluorescence emission is observed. Hamanoue et al. [10] have attributed the very fast ( $10^{-12}$  s) and efficient ( $\Phi_{\text{ph}}=0.9$ ) ISC of F to a favourable spin-orbit coupling due to the dominant  $n, \pi^*$  and  $\pi, \pi^*$  configurations in  $S_1$  and  $T_1$  respectively. In contrast, 3MF shows a very low  $\Phi_{\text{ph}}$  value and, although fluorescence emission is observed ( $\Phi_f=0.03$  in ACN), the overall emission yield is still small (Table 2), indicating a characteristic contribution of the 3-methoxy group to the photophysical properties. Bhat-tacharyya et al. [11] observed that the introduction of a second phenyl group at the 3-position of F results in a complete loss of spectral resolution, an apparent blue shift and a reduction in  $\Phi_{\text{ph}}$ . These workers have proposed that the steric interaction between the two adjacent phenyl groups results in a loss of planarity of the phenyl groups with respect to the enone moiety, and gives rise to a broad potential surface in the ground state due to torsion of the phenyl groups about the single bonds linking them to the enone moiety. Indeed, our  $^{13}\text{C}$  NMR spectra indicate a shielding of C-2 in 3MF relative to F, also observed in the literature [23] for other 3-substituted flavones, as expected for a loss of resonance between the 2-phenyl ring and the chromone unit.

It therefore appears that 3MF shows a distorted structure in the ground state, where the steric repulsion between the 3-methoxy and 2-phenyl substituents rotates these groups out of the benzopyrone plane. Consequently, the reduction in  $\Phi_{\text{ph}}$  of 3MF may be explained by an additional degree of internal conversion of the excited state involving twisting of the 2-phenyl and 3-methoxy groups about the ene double bond. Moreover, the slight activation of fluorescence emission can be attributed to small changes in the relative configurations and the energetic proximity of  $S_1$  and  $T_1$ , reducing the ISC efficiency. However, these arguments cannot explain the strong reduction in  $\Phi_{\text{ph}}$  caused by 3-methoxy substitution, indicating an additional non-radiative deactivation channel from either the triplet or singlet state of 3MF.

### 4.2. Transients from flash photolysis

#### 4.2.1. F and 7MF

The nature of the transients observed by nanosecond flash photolysis depends critically on the position of the methoxy substituent. F and 7MF generate transient species with a quenching behaviour typical of triplet excited states. Transient quenching by oxygen and triplet energy acceptors with energies lower than the estimated triplet energies of the flavones is observed. As expected, transient species with similar

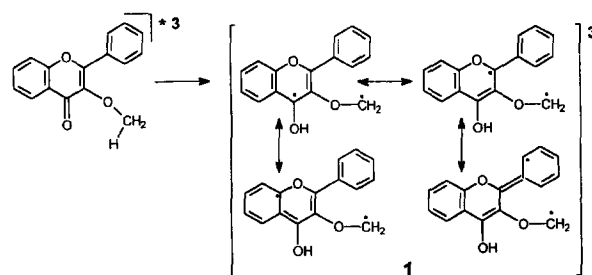
spectra and lifetimes were obtained by energy transfer from triplet BZP ( $E_{T_1} = 69 \text{ kcal mol}^{-1}$ ) [27] to F or 7MF, with bimolecular rate constants close to the diffusion-controlled limit (Table 2). These findings resemble the similarities between F and 7MF observed in the steady state spectroscopic studies, and confirm that the methoxy group at C-7 does not significantly affect the known excited state properties of F.

The observed electron transfer reactivity for the F and 7MF transients is typical of triplet state transients [27]. The small differences in the rate constants ( $k_E$ , Table 2) are in agreement with the similar  $E_{S_1}$  and  $E_{T_1}$  values of these flavones; the somewhat higher  $k_E$  values for 7MF may be related to a more favourable half-wave oxidation potential (estimated as 2.50 eV and greater than 2.80 eV in ACN vs. Ag/AgI for 7MF and F respectively; see Section 2). The modified transient spectra obtained from the quenching of the F and 7MF transients by TCNE and DABCO show long lifetimes (over 50  $\mu\text{s}$ ) and consist of the well-known bands of the radical ions of TCNE (anion radical,  $\lambda_{\text{max}} = 420 \text{ nm}$ ) [33] or DABCO (cation radical,  $\lambda_{\text{max}} = 500 \text{ nm}$ ) [31] and, presumably, the corresponding radical ions of F or 7MF. The absorption regions of the radical ions of F and 7MF are quite similar: 360–370 nm for the anion radicals and 450–460 nm for the cation radicals.

#### 4.2.2. 3MF

The transient generated by irradiation of 3MF at 266 and 355 nm shows a completely distinct behaviour. The biexponential decay in the maximum absorption region indicates the formation of a long-lived intermediate. The short-lived transient, which constitutes the only species observed at the borders of the absorption spectrum, is not quenched by any of the triplet energy acceptors used, but is completely removed by oxygen. The fact that no energy transfer from triplet BZP to 3MF could be observed may be due to the higher triplet energy of 3MF compared with F and 7MF (Table 1). The increase in the  $T_1$  energy of 3MF approximates it to the  $T_1$  energy of BZP, resulting in a higher probability of reverse energy transfer, although the sensitization results are not completely conclusive.

Taken together, these results strongly suggest that the fast transient is not a triplet excited state. In order to identify this transient, it should be kept in mind that the preferential 3MF excited state deactivation occurs by radiationless pathways. As mentioned above, the small activation of the fluorescence emission may reflect an approximation of the  $T_1$   $n, \pi^*$  to the  $\pi, \pi^*$  configuration, which should lead to a reduction of the ISC efficiency, as the highly efficient ISC of F is believed to be due to different configurations of the  $S_1$  and  $T_1$  states [10]. Simultaneous with the increase in  $n, \pi^*$  character and energy of  $T_1$  in 3MF, the postulated distortion of the molecular structure, caused by steric hindrance between the 2-phenyl and 3-methoxy groups, can promote a geometry favourable for intramolecular hydrogen abstraction (Norrish type II) from the methoxy group via a six-membered cyclic transition state. In fact, it is known that the presence of an ether oxygen atom



Scheme 2. Formation of the triplet 1,4-biradical **1** by methoxy hydrogen abstraction by the carbonyl group in triplet 3MF. Some resonance structures of **1** are shown to illustrate the delocalization of the ketyl radical centre.

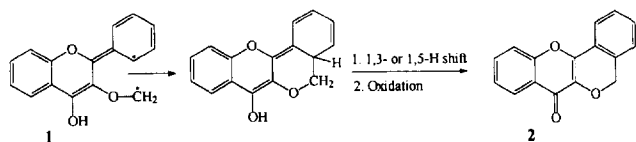
in the  $\beta$ -position relative to the carbonyl group increases the reactivity of the ketone relative to the corresponding alkyl ketone [38].

Therefore, considering the  $\gamma$ -hydrogen abstraction pathway as the main deactivation channel of the 3MF excited state, the fast and slow components of the observed transient can be assigned as a 1,4-biradical intermediate and a product from the intramolecular stabilization reaction of this species respectively (Scheme 2).

The assignment of the biradical structure **1** to the fast transient is in agreement with the quenching by oxygen and the electron donor properties of several biradicals [39,40]. In addition, it is well known that biradicals have absorption properties very similar to the corresponding monoradicals [39–41], and the observed transient spectrum of 3MF, with  $\lambda_{\text{max}}^T = 440 \text{ nm}$ , matches the analogous ketyl radical-like absorption spectrum [41]. On the other hand, the intramolecular reactivity of 3-substituted flavones has been demonstrated by fast intramolecular proton transfer from 3-hydroxy-substituted derivatives ( $k_H \sim 10^{11}–10^{12} \text{ s}^{-1}$ ) [42]. The intermolecular hydrogen abstraction from amines by the  $T_1$  state of F with a bimolecular rate constant of  $k_H \sim 10^7–10^9 \text{ M}^{-1} \text{ s}^{-1}$  has also been reported recently [12]. However, it should be mentioned that, in this intermolecular reaction, a transient spectrum with  $\lambda_{\text{max}}^T = 370 \text{ nm}$  was assigned to a flavone ketyl radical-like intermediate.

At this point, we should briefly comment on the spin multiplicity of the excited state giving rise to the 1,4-biradical. Although the reduction in the ISC efficiency of 3MF may increase the role of  $S_1$  in the photophysical deactivation of 3MF, the lifetime of a hypothetical singlet biradical, arising from  $S_1$  hydrogen abstraction, should certainly be much shorter than the experimentally observed value of 4  $\mu\text{s}$  for the fast transient [40]. Moreover, this reduction in the ISC rate of 3MF is probably not large, as in studies with the analogous 3-phenylflavone,  $\Phi_T = 0.5$  was obtained [11]. Unfortunately, this study did not report the fluorescence behaviour of 3-phenylflavone. Although the observed lifetime is surprisingly long, even for a triplet biradical, the triplet biradical lifetime is controlled by the ISC rate [40], and the geometrical modifications, due to hydrogen abstraction from the methoxy group as well as conjugation of the unpaired electrons, may lead to a higher singlet–triplet splitting and, consequently, to a reduced ISC rate. These effects have been





Scheme 3. Formation of the main photoproduct from the 3MF 1,4-biradical **1**.

used to explain the increased lifetimes of triplet naphthoquinodimethane biradicals and triplet biradicals generated by photoenolization reactions [40]. Therefore it appears that the short-lived transient of 3MF corresponds to the triplet 1,4-biradical **1**.

#### 4.3. Photolysis studies on 3MF

The preliminary results of conventional photolysis confirm the occurrence of a biradical intermediate. The NMR spectrum of the photolysis product mixture clearly indicates the disappearance of the methoxy group and the appearance of an ethereal methylene group. Therefore biradical **1** appears to undergo intramolecular radical coupling, which may occur by ring closure at C-2 or C-4, leading to four-membered oxetane ring structures, or at C-2' of the 2-phenyl group, with the formation of a more stable six-membered ring. The latter possibility appears to be the most probable, as preliminary molecular mechanics calculations indicate the proximity of the O-CH<sub>2</sub> radical centre to the 2'-position of the phenyl ring [37]. The initially formed product re-aromatizes by a 1,3- or 1,5-H shift and may suffer air oxidation to yield the product **2** (Scheme 3).

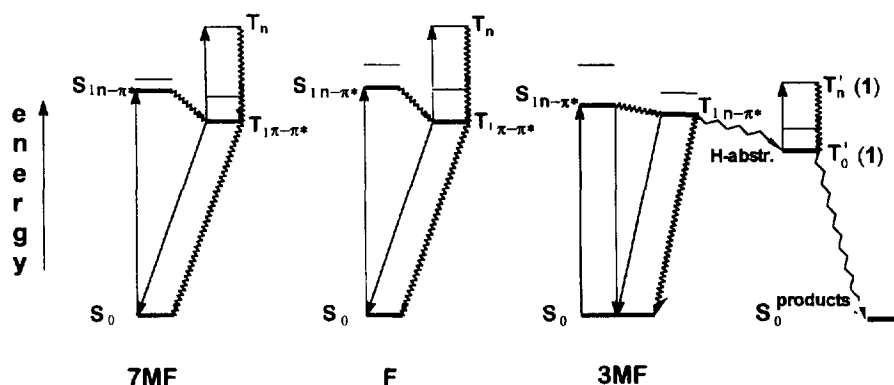
The <sup>13</sup>C NMR spectrum of the partially purified main photoproduct shows the presence of a carbonyl carbon (170.3 ppm) and an ethereal methylene carbon (67.0 ppm). No other signals of saturated carbons are present, excluding several other possible products and indicating the occurrence of re-aromatization and oxidation. The <sup>13</sup>C NMR spectrum is in agreement with the proposed structure **2** (Scheme 3; for assignments, see Section 2), although it shows some signals due to unidentified impurities. In addition, the <sup>1</sup>H NMR spectrum of the photoproduct indicates the occurrence of a substitution at the 2-phenyl ring (see Section 3).

Furthermore, the photolysis product mixture, as well as the partially purified main photoproduct, show absorption spectra similar to 3MF. The slight bathochromic shift (Fig. 6) may indicate a higher degree of delocalization, as expected for the constrained structure **2**. Altogether, these results indicate that the proposed structure **2** is the most probable main photoproduct structure.

## 5. Conclusions

The presence of a methoxy group in flavones introduces different contributions to the photophysical behaviour of these compounds (Scheme 4). A methoxy group in the 7-position leads to an increase in the  $\pi, \pi^*$  character of the excited state, but does not change significantly either the energy levels or the known flavone deactivation pathways. This behaviour is demonstrated by the similar high triplet quantum yields and the reactivity of the triplet state transients, as detected by flash photolysis. In the latter, this study shows the efficient electron transfer reactivity of the triplet states of F and 7MF.

In contrast, a methoxy group in the 3-position leads to a strong geometric constraint, which promotes a decrease in the  $\pi, \pi^*$  character of the excited states, concomitant with an increase in the  $n, \pi^*$  character and triplet state energy level. Moreover, the methoxy group in 3MF becomes available as an intramolecular hydrogen donor for the triplet carbonyl group. The low radiative quantum yield of 3MF is suggestive of a preferential non-radiative deactivation pathway. In agreement, the short-lived transient observed by laser flash photolysis does not show excited state characteristics. Furthermore, the spectral and electron donor properties of this transient are compatible with a 1,4-biradical structure, formed by intramolecular hydrogen abstraction by the triplet excited carbonyl group from the methoxy moiety. Conventional photolysis indicates the transformation of the methoxy group into an ethereal methylene group, as expected for a product resulting from the biradical intermediate **1** (Scheme 2 and Scheme 3).



Scheme 4. Comparison of the photophysical properties of the flavones. In 3MF, the T<sub>0</sub> state of the biradical **1** (T<sub>0</sub>(**1**)) is formed by hydrogen abstraction from the 3-methoxy group.

The photophysical properties exhibited by the flavones studied may be relevant to the biological role of naturally occurring flavonoids. Moreover, recent studies with polymethoxylated flavones have also demonstrated the unusual behaviour of 3-methoxy-substituted derivatives [43].

### Acknowledgements

We thank the CNPq, FAPESP and FINEP Foundations for financial support. We are grateful to Dr. F.H. Quina for critical reading of the manuscript and Dr. N.F. Roque for helpful discussions. Special thanks are extended to Dr. M.J. Politi for valuable advice concerning the laser flash experiments.

### References

- [1] M.M. Caldwell, in A.C. Giese (ed.), *Photophysiology*, Vol. VI, Academic Press, New York, 1971, pp. 131–177.
- [2] J.B. Harborne and T.W. Goodwin (eds.), *Plant Pigments*, Academic Press, Oval Road, London, 1987.
- [3] L. Jurd, in T.A. Geissmann (ed.), *The Chemistry of Flavonoid Compounds*, MacMillan, New York, 1962.
- [4] J.W. McClure, in J.B. Harborne and T.J. Mabry (eds.), *The Flavonoids*, Chapman and Hall, London, 1975.
- [5] H. Mohr, in R.E. Kendrick and G.H. Kronenberg (eds.), *Photomorphogenesis in Plants*, Martinus Nijhoff, Dordrecht, 1986.
- [6] H.A. Stafford, *Plant Physiol.*, **96** (1991) 680.
- [7] M.I. Wilson and B.M. Greenberg, *Photochem. Photobiol.*, **53** (1993) 845.
- [8] I. Yokoe, M. Tagushi, Y. Shirataki and M. Komatsu, *J. Chem. Soc., Chem. Commun.*, (1979) 333.
- [9] M. Monici, N. Mulinacci, P. Baglioni and F.F. Vincieri, *J. Photochem. Photobiol. B: Biol.*, **20** (1993) 167, and references cited therein.
- [10] K. Hamanoue, T. Nakayama, T. Miyake and H. Teranishi, *Chem. Lett.*, (1981) 39.
- [11] K. Bhattacharyya, D. Ramaiah, P.K. Das and M.V. George, *J. Phys. Chem.*, **90** (1986) 5984.
- [12] V. Avila and C.M. Previtali, *J. Chem. Soc., Perkin Trans.*, **2** (1995) 228.
- [13] T. Matsuura, T. Takemoto and R. Nakashima, *Tetrahedron Lett.*, **19** (1971) 1539.
- [14] M. Itoh, Y. Tanimoto and K. Tokumura, *J. Am. Chem. Soc.*, **105** (1983) 3339.
- [15] M. Itoh, Y. Fujiwara, M. Sumitani and K. Yoshihara, *J. Phys. Chem.*, **90** (1986) 5672.
- [16] D. McMorro and M. Kasha, *J. Phys. Chem.*, **88** (1984) 2235.
- [17] M.L. Martinez, S.L. Studer and P.T. Chou, *J. Am. Chem. Soc.*, **112** (1990) 2427.
- [18] K. Tokumura, N. Ygata, Y. Fujiwara and M. Itoh, *J. Phys. Chem.*, **97** (1993) 6656.
- [19] M.L. Martinez, S.L. Studer and P.T. Chou, *J. Am. Chem. Soc.*, **113** (1991) 5881.
- [20] H. Mukaihata, T. Nagakawa, S. Kohtani and M. Itoh, *J. Am. Chem. Soc.*, **116** (1994) 10 612.
- [21] P. Wang and S. Wu, *J. Photochem. Photobiol. A: Chem.*, **77** (1994) 127.
- [22] D.D. Perrin, W.L.F. Armarego and D.R. Perrin, *Purification of Laboratory Chemicals*, Pergamon, London, 2nd edn., 1980.
- [23] P.K. Agrawal and R.P. Rastogi, *Heterocycles*, **16** (1981) 2181.
- [24] M.S. Baptista, I. Cuccovia, H. Chairnovich and M.J. Politi, *J. Phys. Chem.*, **96** (1992) 6442.
- [25] S.M. Ormson, R.G. Brown, F. Vollmer and W.J. Rettig, *J. Photochem. Photobiol. A: Chem.*, **81** (1994) 65.
- [26] I. Carmichael, W.P. Helman and G.L. Hug, *J. Phys. Chem. Ref. Data*, **16** (1987) 239.
- [27] S.L. Murov, I. Carmichael and G.L. Hug, *Handbook of Photochemistry*, Marcel Dekker, New York, 1993.
- [28] A.A. Gorman, I.R. Gould and I. Hamblett, *J. Am. Chem. Soc.*, **103** (1981) 4553.
- [29] S.L. Murov, *Handbook of Photochemistry*, Marcel Dekker, New York, 1973.
- [30] T.M. McKinney and D.H. Gerske, *J. Chem. Soc.*, **87** (1965) 3013.
- [31] K. Bhattacharyya and P.K. Das, *J. Phys. Chem.*, **90** (1986) 3987.
- [32] M.E. Peover, *Trans. Faraday Soc.*, **58** (1962) 2370.
- [33] N. Mataga, Y. Kanda and T. Okada, *J. Phys. Chem.*, **90** (1986) 3882.
- [34] T. Osa and T. Kuwana, *J. Electroanal. Chem.*, **22** (1969) 389.
- [35] E.M. Kosower and J.L. Cotter, *J. Am. Chem. Soc.*, **86** (1964) 5524.
- [36] J.B. Gallivan and J.S. Brinen, *Chem. Phys. Lett.*, **10** (1971) 455.
- [37] M. Christoff, J.P.S. Farah and W.J. Baader, in preparation.
- [38] F.D. Lewis and N.J. Turro, *J. Am. Chem. Soc.*, **92** (1970) 311.
- [39] R.D. Small, Jr. and J.C. Scaiano, *J. Phys. Chem.*, **81** (1977) 828.
- [40] L.J. Johnston and J.C. Scaiano, *Chem. Rev.*, **89** (1989) 521.
- [41] H. Lutz, E. Bréhéret and L. Lindqvist, *J. Phys. Chem.*, **14** (1973) 1758.
- [42] G.A. Brucker, T.C. Swinney and D.F. Kelley, *J. Phys. Chem.*, **95** (1991) 3190.
- [43] M. Christoff, M. Kato, V.G. Toscano and W.J. Baader, in preparation.